ICCK

Journal of Nonlinear Dynamics and Applications
http://dx.doi.org/10.62762/JNDA.2025.493957

RESEARCH ARTICLE

Check for updates

State-Dependent Intermittent Synchronization Control for Coupled Switched Neural Networks: A Prescribed-Time Approach

Yu Yao[1] **and Changqing Long**[2,*]

[1] Southwest Guizhou Vocational and Technical College for Nationalities, Xingyi 562400, China
[2] College of Control Science and Engineering, Zhejiang University, Hangzhou 310027, China

Abstract

This paper addresses the problem of achieving prescribed-time synchronization of coupled switched neural networks (CSNNs) using state-dependent intermittent control. Unlike traditional intermittent control, the intervals for work and rest in this approach are not pre-designed but determined by the relationship between the designed Lyapunov function and the boundary auxiliary functions. The proposed control strategy can effectively mitigate chattering behavior arising from rapid switching in traditional intermittent control. Subsequently, leveraging Lyapunov theory and various inequality techniques, we develop a new set of sufficient conditions, formulated as linear matrix inequalities (LMIs), to ensure prescribed-time synchronization of CSNNs under the designed intermittent control strategy. In the end, a numerical example is given to verify the obtained theoretical results.

Keywords: coupled switched neural networks, intermittent control, prescribed-time synchronization, Lyapunov function, linear matrix inequalities.

Submitted: 30 June 2025
Accepted: 03 August 2025
Published: 24 August 2025

Vol. 1, **No.** 1, 2025.
10.62762/JNDA.2025.493957

***Corresponding author:**
✉ Changqing Long
lcqzju@zju.edu.cn

1 Introduction

Complex networks consist of a large number of nodes, with each node being a fundamental element within the networks. There exist complex relationships and topological structures among these nodes. As a result, its dynamic behaviors become more complicated and challenging to handle [1]. Practical applications like public transportation networks, power systems, and the Internet heavily rely on the dynamic behavior of networks [2], such as stability and synchronization. Thus, the dynamical analysis of complex networks has garnered significant attention from scholars in recent years. CSNNs, as a special type of complex networks, and their synchronization behavior also play an important role in the fields of secure communication [3], and information processing [2].

In previous synchronization analyses of coupled neural networks (CNNs) with or without state-dependent switching connection weights, including asymptotic synchronization [2, 4], finite-time synchronization [5, 6], and fixed-time synchronization [7], these synchronization results have their limitations. Specifically, asymptotic synchronization requires the system to converge

Citation
Yao, Y., & Long, C. (2025). State-Dependent Intermittent Synchronization Control for Coupled Switched Neural Networks: A Prescribed-Time Approach. *Journal of Nonlinear Dynamics and Applications*, 1(1), 3–9.

as time tends to positive infinity. For finite-time synchronization, the settling time is dependent on the initial state of the system. In CSNNs, however, the estimation of the initial error may be inaccurate due to switching behaviors and the complexity of the coupling structure, further affecting the predictability of the settling time. While the settling time of fixed-time synchronization is theoretically independent of the initial values, it is still determined by the parameters of the controller. The switching behaviors and coupling nonlinearities in CSNNs make parameter design more complex, rendering it challenging to balance convergence speed with control intensity.

On the other hand, the settling time for fixed-time synchronization is not affected by initial values but still depends on the control parameters. In practical applications, it is often preferable for the settling time to be independent of any parameters and to be adjustable according to demand [8]. Consequently, it is essential to investigate the prescribed-time synchronization of CSNNs.

Recently, various types of controllers have been designed, such as discontinuous control [3, 10], smooth control [11], etc. [9, 12], to achieve prescribed-time synchronization of CSNNs or CNNs. It should be pointed out that these works have not involved intermittent control. To the best of the author's knowledge, no relevant works have utilized intermittent control to achieve the prescribed-time synchronization of CSNNs. The most similar work is literature [8], where the authors investigated the prescribed-time stabilization problem of complex networks, but the complex networks are continuous, and the intermittent control is time-dependent, the work and rest intervals need to be designed in advance. Moreover, chattering behaviors may occur in such control [13]. Fortunately, Wang et al. [14] have proposed a new type of intermittent control, known as state-dependent intermittent control, which can effectively address the aforementioned issues. Subsequently, this type of intermittent control has been further improved and extended, and has been used to achieve finite/fixed time stability and quasi-synchronization problems for other nonlinear systems [15–17].

Currently, there are few reported studies on achieving prescribed-time synchronization of CSNNs using state-dependent intermittent control. In order to fill this research gap, this paper designs a new class of state-dependent intermittent control and utilizes it to tackle the prescribed-time synchronization problem of CSNNs. The major contributions are summarized as follows.

1. We propose a novel state-dependent intermittent control method that effectively mitigates the chattering behavior caused by the rapid switching inherent in traditional intermittent control.
2. We derive a novel and easily verifiable criterion in the form of LMIs that guarantees prescribed-time synchronization of CSNNs under the proposed controller.

2 Notation

Throughout the paper, $\Im = \{1, 2, \cdots, N\}$, $\mathcal{R}^n$ represents the n-dimensional Euclidean space; In a symmetric matrix, symmetric elements are denoted by the symbol '$*$', and the transpose of a matrix is represented by the symbol '$\top$'; '$\otimes$' denotes the Kronecker product, and I_n stands for $n \times n$ identity matrix. Define two sets $\Xi_1(\nu_{pi}) = \{\nu_{pi} | |\nu_{pi}| \leq \mathcal{T}_i\}$, $\Xi_2(\nu_{pi}) = \{\nu_{pi} | |\nu_{pi}| > \mathcal{T}_i\}$ with $p \in \Im$, $i = 1, 2, \cdot \cdot \cdot, n$ and $\mathcal{T}_i > 0$ denotes thresholds for state-dependent switching. $\tilde{a}_{ij} = \max\{|a^{\dagger}_{ij}|, |a^{\ddagger}_{ij}|\}$. $\overline{\text{co}}[a_{ij}(\omega_{pi})] = \{a^{\dagger}_{ij}, a^{\ddagger}_{ij}\}$ is the convex hull of $\overline{\text{co}}\{a^{\dagger}_{ij}, a^{\ddagger}_{ij}\}$, $a^{\dagger}_{ij}$ and $a^{\ddagger}_{ij}$ represent the lower and upper bounds of the connection weights respectively.

3 Problem Statement

Based on the previous works [2, 4, 5, 7], a class of CSNNs consisting of N neuron nodes is considered as follows

$$\dot{\nu}_p(t) = -D\nu_p(t) + A(\nu_p(t))f\big(\nu_p(t)\big) + \delta \sum_{q=1}^{N} w_{pq}\Pi\nu_q(t) + u_p(t),\ t \geq 0,\ p \in \mathcal{N}, \quad (1)$$

where $\nu_p(t) = (\nu_{p1}(t), \nu_{p2}(t), \cdot \cdot \cdot, \nu_{pn}(t))^{\top} \in \mathcal{R}^n$ is the state of node p, $D = \text{diag}\{d_1, d_2, \cdot \cdot \cdot, d_n\}$ is a diagonal matrix, where $d_p > 0$ stands for the neuron self-inhibitions, $A(\nu_p(t)) = (a_{ij}(\nu_{pi}))_{n\times n}$, is the switched connection weight matrix and take values as $a^{\dagger}_{i,j}$ if $\nu_{pi} \in \Xi_1(\nu_{pi})$, or otherwise $a^{\ddagger}_{i,j}$ if $\nu_{pi} \in \Xi_2(\nu_{pi})$. $f(\cdot) \in \mathcal{R}^n$ is the activation function. $\Pi = \text{diag}\{\Pi_1, \Pi_2, \cdot \cdot \cdot, \Pi_n\}$ denotes inner coupling matrix. $W = (w_{pq})_{N\times N}$ is the configuration matrix, where its elements are required to satisfy $w_{pq} = w_{qp} (p \neq q)$ and $w_{pp} = -\sum_{q=1,q\neq p}^{N} w_{pq}$, $\delta >$ is a coupling strength. $u_p(t) = (u_{p1}(t), u_{p2}(t), \cdot \cdot \cdot, u_{pn}(t))^{\top} \in \mathcal{R}^n$ denotes control input. To derive the main results of this paper, the activation function is required to satisfy the following assumption

Assumption 1 *For any* $p \in \Im$, *there exists positive constant* M_p *and* L_p *such that*

$$\|f_p(y)\| \leq M_p, \ \|f_p(y) - f_p(x)\| \leq L_p\|y - x\|$$

for $\forall y, x \in \mathcal{R}^n$.

Additionally, the isolated node of network (1) has the following form

$$\dot{\omega}(t) = -D\omega(t) + A(\omega(t))f\big(\omega(t)\big) \tag{2}$$

where $\omega(t) = (\omega_1(t), \omega_2(t), \cdots, \omega_n(t))^\top \in \mathcal{R}^n$.

The synchronization error is defined by $e_p(t) = \nu_p(t) - \omega(t)$. By employing the differential inclusion and measurable selection theorems [18], it follows from (1) and (2) that there exist $\acute{a}_{ij}(t) \in \overline{\text{co}}[a_{ij}(\nu_{pi})]$, $\grave{a}_{ij}(t) \in \overline{\text{co}}[a_{ij}(\omega_{pi})]$, $\overline{\text{co}}[a_{ij}(\nu_{pi})] = \overline{\text{co}}[a_{ij}(\omega_{pi})] = \overline{\text{co}}\{a^{\dagger}_{ij}, a^{\ddagger}_{ij}\}$ such that

$$\begin{aligned}\dot{\boldsymbol{e}}(t) =& \big(-I_N \otimes D + \delta W \otimes \Pi\big)\boldsymbol{e}(t) + \big(I_N \otimes \acute{A}(t)\big)f\big(\boldsymbol{e}(t)\big) \\ &+ [I_N \otimes (\acute{A}(t) - \grave{A}(t))]f\big(\boldsymbol{\omega}(t)\big) + \boldsymbol{u}(t), \end{aligned}\tag{3}$$

where $\boldsymbol{e}(t) = (e_1^\top(t), e_2^\top(t), \cdots, e_N^\top(t))^\top$, $\boldsymbol{u}(t) = (u_1^\top(t), u_2^\top(t), \cdots, u_N^\top(t))^\top$, $f(\boldsymbol{e}(\cdot)) = \big(f^\top(e_1(\cdot)), f^\top(e_2(\cdot)), \cdots, f^\top(e_N(\cdot))\big)^\top$, $f(e_p(\cdot)) = f(\nu_p(\cdot)) - f(\omega_p(\cdot)), p \in \Im$, $\acute{A}(t) = (\acute{a}_{ij}(t))_{n\times n}$, $\grave{A}(t) = (\grave{a}_{ij}(t))_{n\times n}$.

4 Main Results

In this paper, the state-dependent intermittent control is designed as follows

$$\boldsymbol{u}(t) = \begin{cases} \bar{\boldsymbol{u}}(t), & \mathcal{V}(t) \in \Gamma_1(t), \\ 0, & \mathcal{V}(t) \in \Gamma_2(t), \\ \bar{\boldsymbol{u}}(t^-), & \mathcal{V}(t) \in \Gamma_3(t), \end{cases} \tag{4}$$

where $\bar{\boldsymbol{u}}(t) = -(\boldsymbol{K}\otimes I_n)\boldsymbol{e}(t) - \text{sign}(\boldsymbol{e}(t))[\aleph + c\lambda(t)\mathcal{V}(t)]$, $\mathcal{V}(t)$ is the designed Lyapunov function in this paper, $\boldsymbol{K}$ is matrix control gain, $\aleph > 0$, $c > 0$, $\lambda(t) = \frac{T_{pre}}{T_{pre}-t}$, t^- denotes the previous instant of time t, and $\Gamma_1(t) = \{\mathcal{V}(t) \in \mathcal{R}^+ : \mathcal{V}(t) \geq \mathcal{W}_1(t)\}$, $\Gamma_2(t) = \{\mathcal{V}(t) \in \mathcal{R}^+ : \mathcal{V}(t) < \mathcal{W}_2(t)\}$, $\Gamma_3(t) = \{\mathcal{V}(t) \in \mathcal{R}^+ : \mathcal{W}_2(t) \leq \mathcal{V}(t) < \mathcal{W}_1(t)\}$, $\mathcal{W}_j(t) = \beta\mathcal{V}(t_0)\text{exp}\left\{-2c_j\int_{t_0}^{t}\lambda(s)ds\right\}, 0 < \beta < 1, c_j > 0, j = 1, 2$, $c > c_2 > c_1$.

Remark 1 *Conventional periodic intermittent control is typically time-dependent, with its activation time sequences predetermined and unable to adapt to system dynamics. This may lead to resource wastage to some extent in practical applications and may induce chattering. To address this issue, the controller proposed in this paper divides the control region into three parts:* $\Gamma_1(t)$, $\Gamma_2(t)$, *and* $\Gamma_3(t)$, *specifically introducing the transition region* $\Gamma_3(t)$. *This region is situated between* $\Gamma_1(t)$ *and* $\Gamma_2(t)$, *acting as a buffer during control switching. Enlarging the scope of* $\Gamma_3(t)$ *prolongs the dwell time of the system state within this region (i.e., the transition period). This implies that by adjusting controller parameters (such as* c_1, c_2, β*), the switching frequency of the controller can be significantly reduced, thereby effectively suppressing chattering.*

Remark 2 *The presence of auxiliary boundary functions* $\mathcal{W}_1(t)$ *and* $\mathcal{W}_2(t)$ *is crucial, as it helps to prevent the occurrence of chattering phenomenon resulting from rapid switching between control and non-control intervals. While the fundamental concept of using boundary functions to guide intermittent control is inspired by [13, 16], this work represents its first successful theoretical extension and application to address the more challenging problem of prescribed-time synchronization for coupled switched neural networks, which involves a distinct analytical approach to handle the prescribed-time performance objective.*

Remark 3 *The activated mechanism of the state-dependent intermittent controller (4) is described as follows:*

1. *When* $\mathcal{V}(t) \in \Gamma_1(t)$:
   The control input $\boldsymbol{u}(t) = \bar{\boldsymbol{u}}(t)$ *is activated. This occurs when the Lyapunov function value exceeds the upper bound* $\mathcal{W}_1(t)$, *initiating the control period.*
2. *When* $\mathcal{V}(t) \in \Gamma_2(t)$:
   The control input $\boldsymbol{u}(t) = 0$ *is activated (control is turned off). This occurs when the Lyapunov function value falls below the lower bound* $\mathcal{W}_2(t)$, *initiating the rest period.*
3. *When* $\mathcal{V}(t) \in \Gamma_3(t)$:
   The control input inherits the previous state, $\boldsymbol{u}(t) = \boldsymbol{u}(t^-)$.
   This occurs when the Lyapunov function value is in the transition region $[\mathcal{W}_2(t), \mathcal{W}_1(t)]$, *and the control status remains unchanged (either active or inactive).*

Remark 4 *The roles of the parameters involved in the control strategy of this paper are described as follows: Increasing the boundary scaling coefficient* β *or narrowing the boundary layer gap* $c_2 - c_1$ *expands the range of the transition region* $\Gamma_3(t)$, *thereby prolonging the state-switching transients and effectively suppressing high-frequency chattering phenomena; simultaneously, increasing the control gain* c *or reducing the prescribed-time* T_{pre} *significantly enhances the system convergence rate.*

Theorem 1 *Suppose that Assumption 1 holds, if there exist positive constants c, $c_j (j = 1, 2)$, ξ, $\aleph$ and matrix $\boldsymbol{K}$ such that $c > c_2 > c_1$, $\mathcal{J} < \aleph$ and*

$$\begin{bmatrix} \Omega_{11} & I_N \otimes \tilde{A} & \mathcal{L} \otimes I_n \\ * & -2\xi^{-1} I_N \otimes I_n & 0 \\ * & * & -2\xi I_N \otimes I_n \end{bmatrix} \leq 0, \tag{5}$$

where $\mathcal{J} = \max_{1\leq i,j\leq n, 1\leq p\leq N}\{|a_{ij}^{\dagger} - a_{ij}^{\ddagger}|M_p\}$, $\Omega_{11} = -\boldsymbol{K} \otimes I_n - I_N \otimes D + \delta W \otimes \Pi$, $\mathcal{L} = \text{diag}\{L_1, L_2, \cdots, L_N\}$. Then, systems (1) and (2) realize prescribed-time synchronization under the state-dependent intermittent control (4).

Proof. Choose a Lyapunov function candidate as

$$\mathcal{V}(t) = \sqrt{\boldsymbol{e}^{\top}(t)\boldsymbol{e}(t)},\ \boldsymbol{e}(t) \in \mathcal{R}^{nN} \backslash \{0\}, \tag{6}$$

When $\mathcal{V}(t) \in \Gamma_1(t)$, calculating the derivative of $\mathcal{V}(t)$ along the trajectory of system (3) gives

$$\begin{aligned} \frac{d\mathcal{V}(t)}{dt} \leq & \frac{\boldsymbol{e}^{\top}(t)}{\mathcal{V}(t)}\Big[\big(-\boldsymbol{K} \otimes I_n - I_N \otimes D \\ & + \delta W \otimes \Pi\big)\boldsymbol{e}(t) + \big(I_N \otimes \acute{A}(t)\big) f\big(\boldsymbol{e}(t)\big) \\ & + [I_N \otimes (\acute{A}(t) - \grave{A}(t))] f\big(\boldsymbol{\omega}(t)\big)\Big] \\ & - \aleph - c\lambda(t)\mathcal{V}(t). \end{aligned} \tag{7}$$

By utilizing inequality $\mathcal{X}^{\top}\mathcal{Y} + \mathcal{Y}^{\top}\mathcal{X} \leq \xi\mathcal{X}^{\top}\mathcal{X} + \xi^{-1}\mathcal{Y}^{\top}\mathcal{Y}$ $(\xi > 0)$ and Assumption 1, we get

$$\begin{aligned} & \boldsymbol{e}^{\top}(t)\big(I_N \otimes \acute{A}(t)\big) f\big(\boldsymbol{e}(t)\big) \\ = & \frac{1}{2}[\boldsymbol{e}^{\top}(t)\big(I_N \otimes \acute{A}(t)\big) f\big(\boldsymbol{e}(t)\big) \\ & + f^{\top}\big(\boldsymbol{e}(t)\big)\big(I_N \otimes \acute{A}^{\top}(t)\big)\boldsymbol{e}(t)] \\ \leq & \frac{1}{2}\xi\boldsymbol{e}^{\top}(t)\big(I_N \otimes \acute{A}(t)\big)\big(I_N \otimes \acute{A}^{\top}(t)\big)e(t) \\ & + \frac{1}{2\xi} f^{\top}\big(\boldsymbol{e}(t)\big) f\big(\boldsymbol{e}(t)\big) \\ = & \frac{1}{2}\xi\boldsymbol{e}^{\top}(t)\big(I_N \otimes (\acute{A}(t)\acute{A}^{\top}(t))\big)e(t) + \frac{1}{2\xi}\|f\big(\boldsymbol{e}(t)\big)\|^2 \\ = & \frac{1}{2}\xi e^{\top}(t)\big(I_N \otimes \tilde{A}\tilde{A}^{\top}\big)e(t) + \frac{1}{2}\xi^{-1}e^{\top}(t)\big(\mathcal{L}^2 \otimes I_n\big)e(t) \end{aligned}$$

Equation (7) is equivalent to

$$\begin{aligned} \frac{d\mathcal{V}(t)}{dt} \leq & \frac{\boldsymbol{e}^{\top}(t)}{\mathcal{V}(t)}\Bigg[-\boldsymbol{K} \otimes I_n - I_N \otimes D + \delta W \otimes \Pi \\ & + \frac{1}{2}\left(\xi I_N \otimes \tilde{A}\tilde{A}^{\top} + \xi^{-1}\mathcal{L}^2 \otimes I_n\right)\Bigg]\boldsymbol{e}(t) \\ & - \aleph + \mathcal{J} - 2c\lambda(t)\mathcal{V}(t), \end{aligned}$$

where $\mathcal{J} = \max_{1\leq i,j\leq n, 1\leq p\leq N}\{|a_{ij}^{\dagger} - a_{ij}^{\ddagger}|M_p\}$. Then, the following inequality (8) holds

$$\frac{d\mathcal{V}(t)}{dt} \leq -2c\lambda(t)\mathcal{V}(t), \tag{8}$$

if and only if $-\aleph + \mathcal{J} < 0$ and

$$\begin{aligned} & -\boldsymbol{K} \otimes I_n - I_N \otimes D + \delta W \otimes \Pi \\ & + \frac{1}{2}\Big(\xi I_N \otimes \tilde{A}\tilde{A}^{\top} + \xi^{-1}\mathcal{L}^2 \otimes I_n\Big) \leq 0. \end{aligned} \tag{9}$$

According to Schur's complement, inequality (9) holds if and only if condition (5) is satisfied.

By integrating (8) from t_0 to t, we obtain

$$\mathcal{V}(t) \leq \mathcal{V}(t_0)\text{exp}\left\{-2c\int_{t_0}^{t}\lambda(s)ds\right\}. \tag{10}$$

Note that $0 < \beta < 1$, $\mathcal{V}(t_0) > \mathcal{W}_1(t_0)$. At time t_0, the control input $\bar{\boldsymbol{u}}(t)$ is activated. Due to $c > c_1$, the convergence rate of $\mathcal{V}(t)$ is faster than that of the boundary function $\mathcal{W}_1(t)$. Consequently, there exists a time instant t_1, such that $\mathcal{V}(t_1) = \mathcal{W}_1(t_1)$, i.e., the trajectory of $\mathcal{V}(t)$ intersects $\mathcal{W}_1(t)$ at t_1. Afterwards, the controller $\bar{\boldsymbol{u}}(t)$ remains active according to the designed control strategy, and the trajectory of $\mathcal{V}(t)$ will enter the region defined by Γ_3. Since $c > c_2$, there exists a time instant s_1, such that $\mathcal{V}(s_1) = \mathcal{W}_2(s_1)$, indicating that the trajectory of $\mathcal{V}(t)$ intersects $\mathcal{W}_2(t)$ at s_1. At the same time, control input $\boldsymbol{u}(t) = 0$ is activated, and after time s_1, the trajectory of $\mathcal{V}(t)$ will enter the region defined by Γ_2. Furthermore, the trajectory of $\mathcal{V}(t)$ will again reach the boundary of $\mathcal{W}_1(t)$ at time t_2, activating controller $\bar{\boldsymbol{u}}(t)$, and triggering controller $\boldsymbol{u}(t) = 0$ at time s_2. By repeating the same process, we can obtain the activation instant sequence $t_k (k \in Z^+)$ and the stopping instant sequence $s_k (k \in Z^+)$ of the controller $\boldsymbol{u}(t)$ determined by the relationship between $\mathcal{V}(t)$ and $\mathcal{W}_j(t), j = 1, 2$.

For the sake of theoretical analysis, let $T_c = \bigcup_{k=0}^{\infty}[t_k, s_k)$ and $T_{uc} = \bigcup_{k=0}^{\infty}[s_k, t_{k+1})$ denote the work time and rest time of the controller, respectively. For any $t \in [t_k, s_k) \subset T_c$, it follows from (10) that

$$\begin{aligned} \mathcal{V}(t) \leq & \mathcal{V}(t_k)\text{exp}\left\{-2c\int_{t_k}^{t}\lambda(s)ds\right\} \\ \leq & \mathcal{V}(t_k)\text{exp}\left\{-2c_1\int_{t_k}^{t}\lambda(s)ds\right\}. \end{aligned} \tag{11}$$

Based on the above analysis, when $t = t_k$, one has

$$\mathcal{V}(t_k) = \mathcal{W}_1(t_k) = \beta\mathcal{V}(t_0)\text{exp}\left\{-2c_1\int_{t_0}^{t_k}\lambda(s)ds\right\}. \tag{12}$$

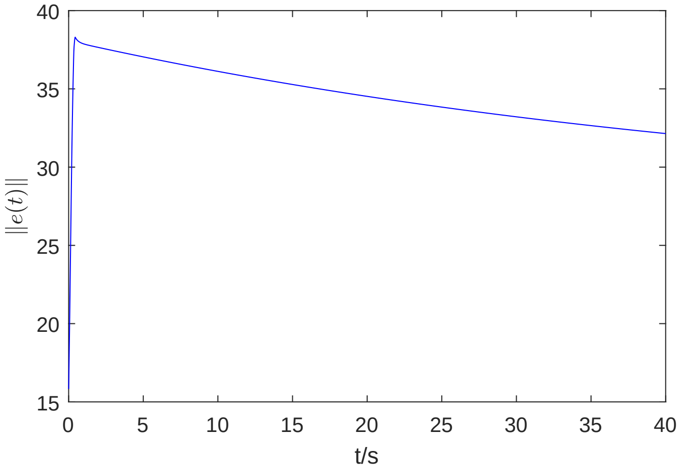

Figure 1. Synchronization error evolution of system (3) without control.

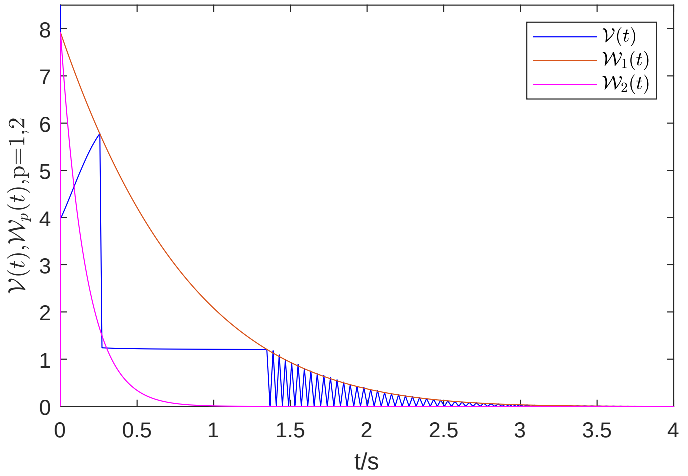

Figure 2. Evolution of $\mathcal{V}(t), \mathcal{W}_1(t)$ and $\mathcal{W}_2(t)$.

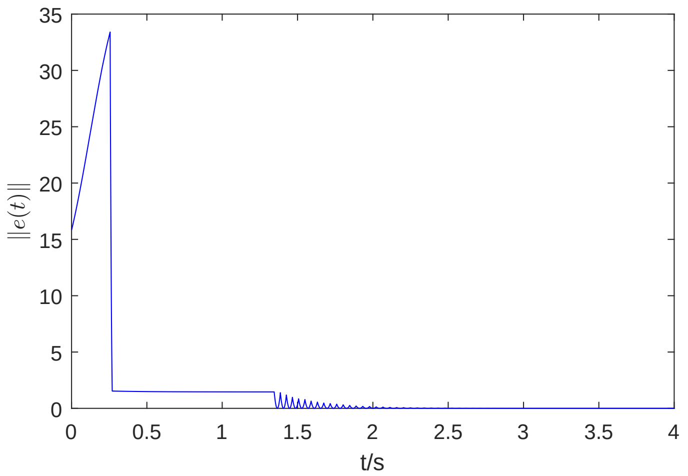

Figure 3. Synchronization error evolution of system (3) with control (4).

Substituting (12) into (11), it gives

$$\mathcal{V}(t) \leq \beta\mathcal{V}(t_0)\text{exp}\left\{-2c_1\int_{t_0}^{t}\lambda(s)ds\right\}, \ t \in [t_k, s_k). \tag{13}$$

When $t \in [s_k, t_{k+1}) \subset T_{uc}$, the trajectory of $\mathcal{V}(t)$ stays in Γ_2 or Γ_3, thus, we can directly obtain the following inequality

$$\mathcal{V}(t) \leq \mathcal{W}_1(t) = \beta\mathcal{V}(t_0)\text{exp}\left\{-2c_1\int_{t_0}^{t}\lambda(s)ds\right\}. \tag{14}$$

It follows from (13) and (14) that

$$\begin{aligned}\mathcal{V}(t) \leq&\beta\mathcal{V}(t_0)\text{exp}\left\{-2c_1\int_{t_0}^{t}\lambda(s)ds\right\}\\ =&\beta\mathcal{V}(t_0)\text{exp}\left\{2c_1T_{pre}\text{ln}\frac{T_{pre}-t}{T_{pre}-t_0}\right\},\end{aligned} \tag{15}$$

for any $t \in [t_0, T_{pre})$. Then, from inequality (15), it can be easily deduced that $\lim_{t\to T_{pre}}\mathcal{V}(t) = 0$, which implies $\lim_{t\to T_{pre}}\|\boldsymbol{e}(t)\| = 0$. According to the definition of prescribed time stability, given in [8], we know that systems (1) and (2) realize prescribed-time synchronization under the state-dependent intermittent control (4). The proof is completed.

5 Numerical Example

This section provides a numerical example to verify the efficiency of the proposed approach.

Example 1 *Consider network (1) with 5 nodes, and $\nu_p(t) = (\nu_{p1}(t), \nu_{p2}(t), \nu_{p3}(t))^\top \in \mathcal{R}^3$ for $p \in \Im$. In addition, the remaining parameters of network (1) are as follows: $D = 0.01I_3$, $\Pi = I_3$, $w_{pq} = 0.6(p \neq q)$, coupling strength $\delta = 0.8$, the activation function $f(\nu) = 0.5(|\nu+1| - |\nu-1|)$ and $\mathcal{T}_1 = \mathcal{T}_2 = 1$, $a^\dagger_{11} = -0.5$, $a^\ddagger_{11} = -0.6$, $a^\dagger_{12} = 3$, $a^\ddagger_{12} = 5$, $a^\dagger_{13} = 2.8$, $a^\ddagger_{13} = 3$; $a^\dagger_{21} = 2$, $a^\ddagger_{21} = 1.9$, $a^\dagger_{22} = -1.7$, $a^\ddagger_{22} = -0.02$, $a^\dagger_{23} = 1.2$, $a^\ddagger_{23} = 1.0$; $a^\dagger_{31} = 1.9$, $a^\ddagger_{31} = 2.6$, $a^\dagger_{32} = 1.5$, $a^\ddagger_{32} = 1.7$, $a^\dagger_{33} = -1.5$, $a^\ddagger_{33} = -1$; Let $\|e(t)\| = \sum_{p=1}^{N} e_p^\top(t)e_p(t)$, and the initial values are set as $\nu_{pi}(0) \in [-1, 1], p \in \Im, i = 1, 2, 3$, $\omega(0) = (1, 2, 1)^\top$. The synchronization results of CSNNs (1) with the given parameters are shown in Figure 1, it can be observed that synchronization of CSNNs (1) cannot be achieved without control.*

Using the LMI tool in MATLAB, the control gains $\boldsymbol{K} = (k_{pq})_{N\times N}$ can be obtained by solving LMI (5) in Theorem 1, where $k_{pp} = 32.2882$, $k_{pq} = 0(p \neq q)$. Additionally, the parameters of controller (4) are selected as $\aleph = 7$, $c = 6$, $c_1 = 0.6$, $c_2 = 3$, $\beta = 0.5$ $T_{pre} = 5s$. The controller parameters ($\aleph = 7, c = 6, c_1 = 0.6, c_2 = 3, \beta = 0.5$)were selected to satisfy the LMI conditions in Theorem 1 while ensuring adequate stability margins *and simulation performance. Figure 2 illustrates the relationship between the trajectories of $\mathcal{V}(t), \mathcal{W}_1(t)$ and $\mathcal{W}_2(t)$, which is consistent with the theoretical analysis presented in this paper. Figure 3 depicts the evolution of the synchronization error of system (3) with control (4). Clearly, the synchronization error $\|e(t)\|$ converges to 0 within the settling time $T_{pre} = 5s$, which means that systems (1) and (2) realize the prescribed-time synchronization. At this point, the validity of the results presented in this paper has been confirmed.*

6 Conclusion

In this paper, a new type of intermittent control has been developed to achieve the prescribed-time synchronization for CSNNs. In this intermittent control strategy, the intervals for work and rest are determined by the relationship between the designed Lyapunov function $\mathcal{V}(t)$ and the boundary functions $\mathcal{W}_1(t)$ and $\mathcal{W}_2(t)$, without the need for pre-designed. In addition, sufficient conditions given in the form of LMIs are derived to guarantee the synchronization of CSNNs within a preset settling time T_{pre}. In the end, numerical results verified the correctness of the theoretical results of this paper.

Data Availability Statement

Data will be made available on request.

Funding

This work was supported without any funding.

Conflicts of Interest

The authors declare no conflicts of interest.

Ethical Approval and Consent to Participate

Not applicable.

References

[1] Wang, X., Cao, J., Yang, B., & Chen, F. (2022). Fast fixed-time synchronization control analysis for a class of coupled delayed Cohen-Grossberg neural networks. *Journal of the Franklin Institute, 359*(4), 1612-1639. [CrossRef]

[2] Zhu, S., & Bao, H. (2022). Event-triggered synchronization of coupled memristive neural networks. *Applied Mathematics and Computation, 415*, 126715. [CrossRef]

[3] Zhao, H., Liu, A., Wang, Q., Zheng, M., Chen, C., Niu, S., & Li, L. (2021). Predefined-time stability/synchronization of coupled memristive neural networks with multi-links and application in secure communication. *Frontiers in Neurorobotics, 15*, 783809. [CrossRef]

[4] Ding, S., & Wang, Z. (2020). Synchronization of coupled neural networks via an event-dependent intermittent pinning control. *IEEE Transactions on Systems, Man, and Cybernetics: Systems, 52*(3), 1928-1934. [CrossRef]

[5] Mei, J., Lu, Z., Hu, J., & Fan, Y. (2020). Guaranteed cost finite-time control of uncertain coupled neural networks. *IEEE Transactions on Cybernetics, 52*(1), 481-494. [CrossRef]

[6] Gong, S., Guo, Z., Wen, S., & Huang, T. (2019). Finite-time and fixed-time synchronization of coupled memristive neural networks with time delay. *IEEE Transactions on Cybernetics, 51*(6), 2944-2955. [CrossRef]

[7] Li, N., Wu, X., Feng, J., Xu, Y., & Lü, J. (2020). Fixed-time synchronization of coupled neural networks with discontinuous activation and mismatched parameters. *IEEE Transactions on Neural Networks and Learning Systems, 32*(6), 2470-2482. [CrossRef]

[8] Chen, T., Liu, X., & Wu, Y. (2023). Prescribed-time stabilization of complex networks with intermittent control. *IEEE Transactions on Circuits and Systems II: Express Briefs, 71*(4), 2069-2073. [CrossRef]

[9] Zhou, X., Cao, J., & Wang, X. (2023). Predefined-time synchronization of coupled neural networks with switching parameters and disturbed by Brownian motion. *Neural Networks, 160*, 97-107. [CrossRef]

[10] Zhou, L., Lin, H., & Tan, F. (2023). Fixed/predefined-time synchronization of coupled memristor-based neural networks with stochastic disturbance. *Chaos, Solitons & Fractals, 173*, 113643. [CrossRef]

[11] Shao, S., Liu, X., & Cao, J. (2021). Prespecified-time synchronization of switched coupled neural networks via smooth controllers. *Neural Networks, 133*, 32-39. [CrossRef]

[12] Bao, Y., Zhang, Y., Zhang, B., & Guo, Y. (2021). Prescribed-time synchronization of coupled memristive neural networks with heterogeneous impulsive effects. *Neural Processing Letters, 53*(2), 1615-1632. [CrossRef]

[13] Wang, Q., He, Y., Tan, G., & Wu, M. (2016, July). Stabilization of linear systems via state-dependent intermittent control. In *2016 35th Chinese Control Conference* (CCC) (pp. 1556-1561). IEEE. [CrossRef]

[14] Wang, Q., He, Y., Tan, G., & Wu, M. (2017). State-dependent intermittent control of non-linear

systems. *IET Control Theory & Applications*, *11*(12), 1884-1893. [CrossRef]

[15] Yu, Z., Yu, S., & Jiang, H. (2023). Finite/fixed-time event-triggered aperiodic intermittent control for nonlinear systems. *Chaos, Solitons & Fractals*, *173*, 113735. [CrossRef]

[16] Song, C., Zhou, J., & Wang, J. (2022). Finite time inter-layer synchronization of duplex networks via event-dependent intermittent control. *IEEE Transactions on Circuits and Systems II: Express Briefs*, *69*(12), 4889-4893. [CrossRef]

[17] Ding, S., Wang, Z., & Zhang, H. (2018). Quasi-synchronization of delayed memristive neural networks via region-partitioning-dependent intermittent control. *IEEE Transactions on Cybernetics*, *49*(12), 4066-4077. [CrossRef]

[18] JAubin, P., & Cellina, A. (1984). Differential Inclusions: Set-Valued Maps and Viability Theory.

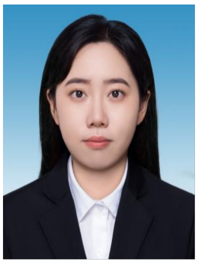

Yu Yao received the M.S. degree in Applied Mathematics from the School of Mathematics and Statistics, South-Central Minzu University, Wuhan, China, in 2024. She is currently serving a faculty member at Southwest Guizhou Vocational and technical college for Nationalities, Xingyi, China. Her current research interests include nonlinear differential algebraic systems, neural networks, and intelligent control. (Email: y_yuuy@163.com)

Changqing Long received the B.S. degree in Applied Mathematics and the M.S. degree in Operational Research and Cybernetics from South-Central Minzu University, Wuhan, China, in 2018 and 2021, respectively. He is currently pursuing a Ph.D. degree in control science and engineering at Zhejiang University, Hangzhou, China. His research interests include edge computing, stability analysis, and machine learning. (Email: lcqzju@zju.edu.cn)